scientific reports

Check for updates

OPEN

The usefulness of different imaging modalities in mandibular osteonecrosis and osteomyelitis diagnosis

Masaya Kawasaki[1], Hiroaki Shimamoto[1]✉, Danielle Ayumi Nishimura[1], Noriko Yamao[1], Naoko Takagawa[1], Yuka Uchimoto[1], Ami Takeshita[1], Tomomi Tsujimoto[1], Sven Kreiborg[2], Sanjay M. Mallya[3], Fan-pei Gloria Yang[1,4,5] & Shumei Murakami[1]

To examine the CT-imaging features of subjects with bacterial osteomyelitis (OM), osteoradionecrosis (ORN), and medication-related osteonecrosis of the jaw (MRONJ) with histopathological confirmation, and to examine the diagnostic efficacy of panoramic radiography and MRI in detecting these disease features. 150 cases with preoperative CT data were selected: 61 bacterial OM, 19 ORN, and 70 MRONJ. 143 cases underwent panoramic X-ray examination, and 47 underwent MRI. The assessment criteria for imaging findings included: (1) bone resorption, (2) osteosclerosis, (3) clarity of the mandibular canal, (4) periosteal reactions, (5) cortical bone perforation, (6) sequestrum, and (7) pathological fractures. CT was considered the gold standard for assessing these features. Compared with CT, all panoramic radiographs were detectable for diagnostic features of the disease. Bone resorption was detected in 123 cases (sensitivity 91.1%), and osteosclerosis was detected in 131 cases (sensitivity 98.5%). With panoramic radiography, most changes to clarity of the mandibular canal and pathological fractures were detected (sensitivities of 87.8% and 68.8%, respectively). However, the sensitivities for detection of periosteal reactions, cortical bone perforation and sequestration were low (19.6%, 17.8% and 19.4%, respectively). Sensitivity of MRI for detecting periosteal reactions, cortical bone perforation, sequestration, and pathological fractures (27.3%, 73.5%, 35.7%, and 60.0%, respectively) was equivalent or superior to panoramic imaging. MR-specific characteristics of bone marrow edema were depicted on almost all examinations. Panoramic radiography may be adequate for identifying bone resorption and osteosclerosis. However, MRI provides more value than panoramic radiography in detecting periosteal reactions, cortical bone perforation, sequestration, and bone marrow edema.

Keywords Osteomyelitis, MRI, Panoramic radiography, CT

Osteomyelitis (OM) is an inflammatory disease of the bone with various etiologies and pathogenetic manifestations[1]. Jawbone OM is common and results from local extension from the skin, oral cavity, or paranasal sinuses[2]. OM frequently occurs in jawbones, and oral and maxillofacial surgeons encounter cases of OM regularly. The incidence of OM in the jawbones is high and is 3–19 times greater in the mandible than in the maxilla[2], particularly in the mandibular molar region[3]. The higher incidence of OM in the mandible is attributed to the thicker cortical bone, which allows inflammation within the bone marrow to progress more easily, and the fact that the blood supply to the mandibular body is primarily only from the inferior alveolar artery[3,4]. Simultaneously, poor blood supply is a contributing factor to intractability. The high frequency of OM in the mandibular molar region also reflects the higher prevalence of local periapical and periodontal inflammation in this region[3]. As OM progresses through the jaws, it causes local bone necrosis and separates bone islands from

[1]Department of Oral and Maxillofacial Radiology, Graduate School of Dentistry, The University of Osaka , 1-8 Yamadaoka, Suita, Osaka 565-0871, Japan. [2]Department of Pediatric Dentistry and Clinical Genetics, School of Dentistry, Faculty of Health and Medical Sciences, University of Copenhagen, Nørre Allé 20, 2200 Copenhagen, Denmark. [3]Section of Oral and Maxillofacial Radiology, UCLA School of Dentistry, 10833 Le Conte Ave., Los Angeles, CA 90095-1668, USA. [4]Department of Foreign Languages and Literature, National Tsing Hua University, No.101, Section 2, Guangfu Rd., East District, Hsinchu 300013, Taiwan. [5]Center for Cognition and Mind Sciences, National Tsing Hua University, No.101, Section 2, Guangfu Rd., East District, Hsinchu 300013, Taiwan. ✉email: shimamoto.hiroaki.dent@osaka-u.ac.jp

the adjacent bone. The dead bone, or sequestrum, is identified on radiographic examination and is a hallmark of chronic suppurative OM.

In contrast, the term "osteonecrosis" refers to a state where the bone becomes devitalized, often occurring without infection, as exemplified by aseptic or avascular necrosis of the femoral head. In the maxilla and mandible, such osteonecrosis may result from prior radiation therapy involving the jaws and is referred to as osteoradionecrosis (ORN), defined as exposed bone that does not heal for more than three months following radiation therapy with no evidence of residual or recurrent tumors, typically occurring with doses of 60 Gy or more to the jawbones[5,6]. Another form of jaw osteonecrosis is associated with antiresorptive therapy, referred to as medication-related osteonecrosis of the jaw (MRONJ). To distinguish it from other forms of osteonecrosis, MRONJ is defined when all three of the following elements are met: (1) Current or previous treatment with antiresorptive therapy alone or in combination with immune modulators or antiangiogenic medications; (2) Exposed bone or bone that can be probed through an intraoral or extraoral fistula(e) in the maxillofacial region that has persisted for more than eight weeks; (3) No history of radiation therapy to the jaws or metastatic disease to the jaws[7].

Practically, distinguishing between OM, ORN and MRONJ is essential. Jawbone OM is predominantly caused by inflammation from bacterial infections (bacterial OM). In contrast, the etiologies of ORN and MRONJ are distinct, although both of these forms of osteonecrosis can become secondarily infected and present with suppuration. However, the extent of necrosis caused by ORN and MRONJ is more extensive, and these forms are often intractable. Therefore, early detection and understanding of the extent of the lesion are crucial to devise an appropriate treatment plan. Radiologic imaging provides key information that can guide decision-making in the diagnosis and management of these diseases[8].

Various imaging techniques, including panoramic radiography and computed tomography (CT), including dental cone-beam CT (CBCT) and MRI, have been applied for the evaluation of jawbone OM, ORN and MRONJ[2]. Additionally, the utility of nuclear medicine examinations such as bone scintigraphy, SPECT/CT, and PET/CT has been reported[9–11]. There is a significant body of literature on imaging diagnostics for jawbone OM, with studies suggesting that CT is more effective than conventional 2D radiography in depicting early abnormalities[12] and is superior in visualizing sequestrum and periosteal reactions[13]. Furthermore, the use of CT volume data allows observation in other planes and enables three-dimensional diagnosis[2]. Owing to these factors, Baba et al.[14] considered CT the gold standard in the imaging diagnosis of jawbone OM, as it accurately depicts the extent of the lesion. Posadzy et al.[15] reported that the diagnostic capabilities of CBCT are equivalent to those of multidetector row CT (MDCT). On the other hand, Lee et al.[16] suggested that MRI is effective for the early detection of jawbone OM.

Although there are numerous reports on the imaging diagnostics of jawbone OM, most studies only clinically diagnose OM, and studies that have evaluated cases where the diagnoses were confirmed by histopathology are scarce. Even in cases where histopathological evidence is available, the number of cases studied is often limited. Furthermore, studies detailing the differences in imaging diagnosis for bacterial OM, ORN, and MRONJ are lacking.

Therefore, this study aims to focus exclusively on cases of bacterial OM, ORN and MRONJ with histopathological confirmation, evaluate their manifestations on CT, panoramic and MRI; and elucidate their efficacy in displaying the characteristic diagnostic manifestations of the disease.

Results

Study patients

Analysis of variance revealed a significant difference in age among patients with different diseases (Table 1, $p < 0.001$). Subsequent post hoc comparisons revealed that the MRONJ group had a significantly greater mean age (75.5 ± 9.9 years) than did the bacterial OM group (64.3 ± 15.5 years), with a p value of < 0.001. No statistically significant differences were detected between the bacterial OM group and the ORN group or between the ORN group and the MRONJ group ($p = 0.087$ and $p = 0.147$, respectively).

Furthermore, a significant difference in sex ratios among the disease groups was identified (Table 1, $p = 0.002$). Upon further investigation between the pairs of groups, the MRONJ group presented a significantly greater percentage of females (53 cases out of 70, 75.7%) than did the ORN group (6 cases out of 19, 31.6%), with a p value of < 0.001. No statistically significant differences were found between the bacterial OM group and the ORN group or between the bacterial OM group and the MRONJ group ($p = 0.019$, $p = 0.096$, respectively). Table 2 shows the original disease information for both the ORN group and the MRONJ group. In addition, Figs. S1–S19

	Bacterial OM (n = 61)	ORN (n = 19)	MRONJ (n = 70)	*p* value
Age (y.o.)				
Mean ± SD	64.3 ± 15.5	71.5 ± 10.7	75.5 ± 9.9	< 0.001
Range	10–85	48–88	45–94	
Sex				
Man	23	13	17	0.002
Woman	38	6	53	

Table 1. Patient demographics. *OM* osteomyelitis, *ORN* osteoradionecrosis, *MRONJ* medication-related osteonecrosis of the jaw.

Original disease	Number of patients
ORN (n = 19)	
Oropharynx cancer	6
Tongue cncer	5
Gingival cancer	3
Cancer of the floor of mouth	2
Submandibular gland cancer	1
Maxillary cancer	1
Cervical lymph node cancer of unknown primary	1
MRONJ (n = 70)	
Osteoporosis	38
Bone metastases from solid tumors	26
Rheumatoid arthritis	4
Multiple myeloma	2

Table 2. Original disease information for ORN and MRONJ patients.

		Bacterial OM (n = 61)	ORN (n = 19)	MRONJ (n = 70)	Total (n = 150)	*p* value
Bone Resorption	+	58 (95.1%)	19 (100%)	65 (92.9%)	142 (94.7%)	0.686
	–	3 (4.9%)	0 (0%)	5 (5.3%)	8 (5.3%)	
Osteosclerosis	+	57 (93.4%)	14 (73.7%)	69 (98.6%)	140 (93.3%)	0.002
	–	4 (6.6%)	5 (26.3%)	1 (1.4%)	10 (6.7%)	
Clarity of the Mandibular Canal	+	56 (91.8%)	10 (52.6%)	63 (90.0%)	129 (86.0%)	< 0.001
	–	5 (8.2%)	9 (47.4%)	7 (10.0%)	21 (14.0%)	
Periosteal Reaction	+	23 (37.7%)	13 (68.4%)	26 (37.1%)	62 (41.3%)	0.037
	–	38 (62.3%)	6 (31.6%)	44 (62.9%)	88 (58.7%)	
Cortical Bone Perforation	+	42 (68.9%)	18 (94.7%)	52 (74.3%)	112 (74.7%)	0.064
	–	19 (31.1%)	1 (5.3%)	18 (25.7%)	38 (25.3%)	
Sequestrum	+	45 (73.8%)	11 (57.9%)	54 (77.1%)	110 (73.3%)	0.242
	–	16 (26.2%)	8 (42.1%)	16 (22.9%)	40 (26.7%)	
Pathological Fracture	+	2 (3.3%)	11 (57.9%)	3 (4.3%)	16 (10.7%)	< 0.001
	–	59 (96.7%)	8 (42.1%)	67 (95.7%)	134 (89.3%)	

Table 3. Presence or absence of each image finding (ratio). *OM* osteomyelitis, *ORN* osteoradionecrosis, *MRONJ* medication-related osteonecrosis of the jaw.

shows radiographic images before and after surgical treatment for the ORN group to facilitate a thorough review of the cases.

CT imaging findings

Table 3 shows the presence or absence (ratios) of each imaging finding examined in this study for the three diseases: 61 bacterial OM, 19 ORN, and 70 MRONJ. Bone resorption was observed in 142 out of 150 cases (94.7%), with no statistically significant difference in the ratio among the three diseases. Osteosclerosis was present in 140 of 150 cases (93.3%), with a statistically significant difference among the three diseases ($p = 0.002$). ORN was not observed in 26.3% of cases, which was more common than MRONJ was ($p = 0.001$), but no statistically significant difference was found compared with bacterial osteomyelitis ($p = 0.031$). Clarity of the mandibular canal was observed in 129 out of 150 cases (86.0%), with a statistically significant difference in the ratio among the three diseases ($p < 0.001$). Clarity of the mandibular canal was lost in 47.4% of ORN cases and was more common than in those with the other two diseases (ORN vs. bacterial OM: $p < 0.001$, ORN vs. MRONJ: $p = 0.001$). Periosteal reactions were observed in 62 out of 150 cases (41.3%), with a statistically significant difference in the ratio among the three diseases ($p = 0.037$). ORN had a frequency of 68.4% (Fig. S20), which was higher than that of MRONJ ($p = 0.015$), but no statistically significant difference was found compared with that of bacterial OM ($p = 0.019$). Cortical bone perforation was observed in 112 out of 150 cases (74.7%), with no statistically significant difference in the ratio among the three diseases. Sequestration was observed in 110 out of 150 cases (73.3%), with no statistically significant difference in the ratio among the three diseases. Pathological fractures were observed in 16 out of 150 cases (10.7%), with a statistically significant difference in the ratio among the three diseases ($p < 0.001$). ORN had a frequency of 57.9%, which was higher than that of the other two diseases (ORN vs. bacterial OM: $p < 0.001$; ORN vs. MRONJ: $p < 0.001$). For all the evaluation items, bacterial OM and MRONJ presented similar observation ratios.

Panoramic radiography

The diagnostic efficacy of panoramic radiography when CT is used as the gold standard is presented in Table 4. When all the evaluation criteria are considered, panoramic radiography can detect radiographic findings in all 143 cases (57 bacterial OM, 19 ORN, and 67 MRONJ), yielding a detection rate of 100%. Among the 135 cases in whom CT revealed bone resorption, panoramic radiography detected bone resorption in 123 cases (91.1%). When CT did not reveal bone resorption, panoramic radiography was also negative, yielding a specificity of 100% and an overall diagnostic accuracy of 91.6% ($p < 0.001$, Table 4). Notably, panoramic imaging did not yield any false-positive results for any of the image evaluation criteria. Panoramic imaging was able to identify osteosclerosis in 131 of the 133 cases (98.5%) with positive CT findings. When CT was negative for osteosclerosis, panoramic imaging was also negative, with a high overall diagnostic accuracy of 98.6% and a significant concordance between the two imaging methods ($p < 0.001$, Table 4). To depict the clarity of the mandibular canal, panoramic radiography had a sensitivity of 87.8%, specificity of 100%, and accuracy of 89.5%, with significant concordance between both imaging methods ($p < 0.001$, Table 4). For identifying periosteal reactions, cortical bone perforations and sequestration, panoramic imaging had low sensitivity (19.6%, 17.8%, and 19.4%, respectively) but 100% specificity, and there was significant concordance between the two imaging methods ($p < 0.001$, Table 4). Pathological fractures were identified on panoramic radiographs with a sensitivity of 68.8%, a specificity of 100%, and a significant concordance between both imaging methods ($p < 0.001$, Table 4).

MRI

The results of the diagnostic performance of MRI when CT was used as the gold standard are presented in Table 5. MRI was able to depict bone resorption and osteosclerosis in only 5 out of 47 cases (20 bacterial OM, 6 ORN, and 21 MRONJ), yielding a detection rate of only 10.6%. The clarity of the mandibular canal outline was discerned in none of the 47 cases, yielding a sensitivity of 0%. The sensitivities of periosteal reactions (27.3%), cortical bone perforation (73.5%) and sequestration (35.7%) were greater than those of panoramic radiography ($p = 0.007$, Table 5). For detecting pathological fractures, MRI had a sensitivity of 60.0%, and significant concordance was observed between the two imaging methods ($p = 0.001$, Table 5).

The results of the evaluation of MR-specific image features are shown in Table 6. On T1-weighted images, the signal intensity of the diseased areas was consistently lower than that of the healthy bone marrow and parotid gland in all 47 cases. Additionally, the signal intensity was approximately equivalent to that of the masseter muscle on the contralateral healthy side. On T2-weighted fat-suppressed images, the signal intensity of the diseased regions was greater than that of the healthy bone marrow, masseter muscle, and parotid gland.

Discussion

The average age of the MRONJ group was more than 10 years greater than that of the bacterial OM group. This is expected—bisphosphonate and denosumab, the driver medications in this disease, are used to treat osteoporosis, bone metastases from malignant tumors, multiple myeloma, etc., which are more common with

			CT		Total	*p* value	Sensitivity (%)	Specificity (%)	Accuracy (%)
			+	−					
Panoramic X-ray Imaging	Bone Resorption	+	123	0	123	<0.001	91.1	100.0	91.6
		−	12	8	20				
	Total		135	8	143				
	Osteosclerosis	+	131	0	131	<0.001	98.5	100.0	98.6
		−	2	10	12				
	Total		133	10	143				
	Clarity of the Mandibular Canal	+	108	0	108	<0.001	87.8	100.0	89.5
		−	15	20	35				
	Total		123	20	143				
	Periosteal Reaction	+	10	0	10	<0.001	19.6	100.0	71.3
		−	41	92	133				
	Total		51	92	143				
	Cortical Bone Perforation	+	19	0	19	0.003	17.8	100.0	38.5
		−	88	36	124				
	Total		107	36	143				
	Sequestrum	+	24	0	24	<0.001	19.4	100.0	44.1
		−	80	39	119				
	Total		104	39	143				
	Pathological Fracture	+	11	0	11	<0.001	68.8	100.0	96.5
		−	5	127	132				
	Total		16	127	143				

Table 4. Diagnostic performance of panoramic X-ray imaging.

			CT		Total	*p* value	Sensitivity (%)	Specificity (%)	Accuracy (%)
			+	−					
MRI	Periosteal Reaction	+	6	0	6	0.007	27.3	100.0	66.0
		−	16	25	41				
	Total		22	25	47				
	Cortical Bone Perforation	+	25	0	25	< 0.001	73.5	100.0	80.9
		−	9	13	22				
	Total		34	13	47				
	Sequestrum	+	10	0	10	0.003	35.7	100.0	61.7
		−	18	19	37				
	Total		28	19	47				
	Pathological Fracture	+	3	0	3	0.001	60.0	100.0	95.7
		−	2	42	44				
	Total		5	42	47				

Table 5. Diagnostic performance of MRI.

		Bacterial OM (n = 20)	ORN (n = 6)	MRONJ (n = 21)	Total (n = 47)	*p* value
T1-wI (Comparison with healthy bone marrow)	Low	20	6	21	47	–
	Intermediate	0	0	0	0	
T1-wI (Comparison with healthy masseter muscle)	Low	3	0	3	6	1.000
	Intermediate	17	6	18	41	
T1-wI (Comparison with healthy parotid gland)	Low	20	6	21	47	–
	Intermediate	0	0	0	0	
T2-wI (Comparison with healthy bone marrow)	Low	0	0	4	4	0.158
	Intermediate	1	0	0	1	
	High	19	6	17	42	
T2-wI (Comparison with healthy masseter muscle)	Low	0	0	1	1	0.318
	Intermediate	0	0	3	3	
	High	20	6	17	43	
T2-wI (Comparison with healthy parotid gland)	Low	0	0	4	4	0.077
	Intermediate	6	0	2	8	
	High	14	6	15	35	

Table 6. Evaluation items by MRI only. *OM* osteomyelitis, *ORN* osteoradionecrosis, *MRONJ* medication-related osteonecrosis of the jaw, *T1-wI* T1-weighted images, *T2-wI* T2-weighted fat-suppressed images, *Low*: low signal intensity, *Intermediate*: intermediate signal intensity, *High*: high signal intensity.

increasing age. Thus, the greater average age in the MRONJ group was attributed to the disease occurrence, which required antiresorptive therapy. In addition, the percentage of females in the MRONJ group was greater than that in the ORN group. This reflects the disease prevalence in Japan. Osteoporosis patients in the MRONJ group have a male-to-female ratio of approximately 1:3.3 in Japan, with a higher prevalence among females[17]. On the other hand, the ORN group consisted of oral and pharyngeal cancer patients, with a male-to-female ratio of approximately 2.3:1 in Japan, indicating a higher prevalence among males[18]. Although the demographics of the disease reflect the local population prevalence, it is similar to the trends of the age- and male-to-female distributions worldwide.

In this study, we used CT results as the gold standard to determine the diagnostic performance of panoramic X-ray imaging and MRI. The sensitivity of CT for diagnosing OM is reported to be 77–78%, with a specificity of approximately 80–86% and an accuracy ranging from 79%[19,20]. However, these reports include few histopathologically confirmed diseases. In some cases, the clinical diagnosis of OM was made with a follow-up of six months or more, whereas in others, radiologists subjectively diagnosed cases as OM without a histopathological diagnosis. These reports indicate that the sensitivity of panoramic X-ray imaging for diagnosing OM is 59%, the specificity is 100%, and the accuracy is 66%[19,20]. Our study design differs from these prior reports—our case inclusion and categorization followed histopathological confirmation of OM or osteonecrosis and established clinical ORN or MRONJ criteria. It is important to note that histopathological confirmation is not applied to routine differential diagnosis of these diseases[21,22]. The distinction between the three entities is based on historic and clinical findings. In our study, the histopathologic confirmation provided confidence that the radiologic manifestations represent the specific disease entity (bacterial OM vs. ORN vs. MRONJ).

In our study, we observed bone resorption and osteosclerosis in more than 90% of the cases, as determined by CT. The diagnostic accuracy of panoramic radiography was also high (91.6% and 98.6%), which is adequate for identifying changes in the lytic and sclerotic changes of OM. Similarly, the accuracy of panoramic radiographs for assessing mandibular canal clarity was 89.5%. In contrast, panoramic radiographs detected only 18% cortical bone perforations and 19% bone sequestration. These features were observed in the majority of the cases (75% and 73% on CT, respectively); thus, panoramic radiography was deemed unsuitable for the detection of these diagnostic manifestations. Similarly, panoramic X-ray imaging revealed that only 20% of periosteal reactions were detected via CT, indicating that it is unsuitable for this diagnostic assessment.

When OM is suspected, conventional X-ray imaging is considered the primary choice for diagnostic imaging[23–26]. Additionally, conventional X-ray imaging is useful for evaluating the progression of the disease by comparing X-ray images at the initial visit with follow-up observations[27]. However, during the acute phase, the presence of OM may be overlooked in conventional X-ray imaging, leading to reported diagnostic accuracy rates of 73%, specificity rates of 81%, and sensitivity rates of 60% in the acute phase[28]. The detection of bone resorption via plain X-ray images requires a decrease in calcium of approximately 30–50%, which is only perceptible 4–8 days after onset. Therefore, abnormal findings may not be evident in the first 2–3 weeks after symptom onset[28]. Although panoramic radiographs enable a comprehensive assessment of structures such as the mandibular canal and maxillary sinus floor, they are limited by blurring of superimposed structures and distortion, and buccolingual information is inferior to that of CT[29]. CT is recognized for providing valuable information on periosteal reactions, cortical bone perforation, and sequestrum, even in cases where abnormal findings are not observed via plain X-ray imaging[28]. CT allows the creation of multiplanar reconstruction images from horizontal sectional images to frontal or sagittal planes, and three-dimensional evaluation of bone resorption, osteosclerosis, cortical bone perforation, and sequestrum is possible[29]. A report comparing surgical findings of MRONJ with CT findings indicated that the range of lesions assessed by CT is underestimated compared with the actual lesion range but shows a significant correlation[30]. In this study, panoramic radiography exhibited low sensitivity in detecting periosteal reactions, cortical bone perforation, and sequestration, as observed with CT, suggesting that the lack of information in the buccolingual dimension was the contributing factor.

Characteristic imaging findings were obtained with MRI; however, the detectability of bone resorption, osteosclerosis, and clarity of the mandibular canal ranged from 0 to 10.6%, which is relatively low. Nevertheless, for periosteal reactions, cortical bone perforation, and osteonecrosis, MRI demonstrated greater sensitivity than panoramic radiography did, suggesting the usefulness of MRI. MRI is considered particularly valuable in detecting the extent of inflammation in the bone marrow[31]. Furthermore, MRI has been reported to show comparable accuracy to CT in diagnosing mandibular OM[32] and is highly sensitive even in the acute phase of the disease before CT can detect morphological changes in the bone. Even in the acute phase, where bone marrow edema (presence of water) leads to low signal intensity in T1-weighted images and high signal intensity in T2-weighted images[28,33,34], MRI has proven to be sensitive in the chronic phase, where the lesion exhibits low signal intensity in both T1- and T2-weighted images due to reduced water content[28]. In T2-weighted fat-suppressed or short-tau inversion recovery sequences, however, the signal from fat is decreased, increasing the visibility of inflammatory changes and fluid collections[24]. The sequestrum is typically depicted as no signal in both T1- and T2-weighted images[35]. However, when MRI findings are compared with surgical observations in MRONJ cases, mixed results of underestimation and overestimation have been reported, with no significant correlation observed[30]. Additionally, dynamic contrast-enhanced bone perfusion analysis via ultrashort echo-time MRI has been reported to be effective in identifying MRONJ[36]. Moreover, reports suggest that the apparent diffusion coefficient values from diffusion-weighted images are useful in distinguishing between acute and chronic OM[37]. It is anticipated that there will be an increasing demand for bone marrow infection imaging diagnosis with MRI in the future.

A comparison of the three conditions revealed that the incidence rates of bacterial OM and MRONJ were similar. Generally, CT and MRI findings in MRONJ are considered nonspecific and resemble those of bacterial OM[38], which is consistent with the results of this study. On the other hand, ORN demonstrated different incidence rates in findings related to osteosclerosis and periosteal reactions than did MRONJ and distinct findings in mandibular canal clarity and pathological fractures compared with the other two conditions. Compared with MRONJ, ORN is characterized by a lower frequency of osteosclerosis and a greater frequency of pathological fractures[39], which aligns with the results of this study. However, while previous studies have suggested that ORN has a lower incidence of periosteal reactions than MRONJ does[39–42], the ORN group had a higher frequency of periosteal reactions than did the MRONJ group in this study. Our sample consisted fewer ORN cases (19), relative to OM (61) and MRONJ (70) subjects. A smaller sample size increases the likelihood of type II error (failing to detect a real effect). Notably, the numbers of ORN cases in two of the prior studies were low[39,40], with 7 and 16 patients and perhaps these studies may not have adequate power to fully detect differences between ORN and MRONJ. In one study[39], periosteal reactions were identified in only 2.9% of MRONJ cases suggesting that differences in recording of periosteal reactions may underly this difference. Future studies with larger sample sizes and metanalyses of existing data may help provide clarity.

One limitation of this study is our defined sample. The inclusion criteria focused exclusively on cases who were diagnosed with OM or osteonecrosis through histopathological examination, which inevitably led to the exclusion of acute bone marrow inflammation or early-stage chronic bone marrow inflammation. In particular, while MRI is known to be extremely sensitive in detecting bone marrow inflammation even in the acute phase before morphological changes are visible on CT, the current study did not specifically investigate the ability of MRI to detect early-stage bone marrow inflammation. Additionally, cases where MRI suggested the possibility of bone marrow inflammation early on, followed by improvement through medication without progressing to histopathological examination, may have been overlooked.

Second, despite conducting a detailed image evaluation of mandibular OM, this study did not assess cases where inflammation spread to soft tissues outside the mandible. With respect to the evaluation of the extent of inflammation spreading to soft tissues, previous reports suggest that MRI has high diagnostic accuracy, followed by MDCT, whereas CBCT evaluations are considered impossible. This limitation is attributed to the absence of CT values in CBCT.

Third, the co-occurrence of ORN and bacterial OM, as well as MRONJ and bacterial OM, has occurred. ORN and stages 1 and below MRONJ are classified as nonbacterial (aseptic) OM in the published literature. The modification of infection that occurs in the tooth and periodontal tissues in areas where bone metabolism and bone immunity are severely compromised, such as by radiation and drugs, leads to bone marrow- and periosteal-derived circulatory failure, resulting in osteonecrosis. At this stage, bacterial infection has not yet occurred, but once bone exposure occurs, bacterial infection can easily occur, leading to the co-occurrence of bacterial OM. Since this study focused only on cases that underwent histopathological examination, which tends to include more advanced cases, it is speculated that there were a considerable number of cases with co-occurrence of ORN and bacterial OM, as well as MRONJ and bacterial OM. Despite these limitations, our study provides an in-depth comparison of the performance of panoramic radiographs and MRI in evaluating a majority of cases of OM/osteonecrosis occurring in the jaw. Future studies should also evaluate the maxilla, where the spectrum of the findings and their frequencies might differ from those in the mandible.

Methods

Subjects

This study was conducted in accordance with the Helsinki Declaration and ethical guidelines for clinical research. Approval was obtained from the Ethics Committee of Graduate School of Dentistry, The University of Osaka (Approval numbers: H21-E16, H21-E16-1, H29-E50, R4-E32). Written informed consent was obtained from all the participants and/or their legal guardians after the nature of the procedures was explained.

The retrospective study period was from January 2010 to August 2023. A total of 2903 cases were identified through a search in the Radiological Imaging Diagnostic Report System of our hospital via the keywords "osteomyelitis" OR "osteonecrosis" OR "ONJ" OR "radiation induced" OR "osteoradio". From the search results, only cases that occurred in the mandibular molar region with histopathological confirmation of OM or osteonecrosis were extracted. The search identified 150 pretreatment CT examinations (including 29 CBCT examinations) where artifacts from dental prostheses or patient motion did not affect the image diagnosis. Among these cases, 143 also had panoramic radiographs, and 47 cases had pretreatment MR images. The breakdown of the study participants is presented in Table 1.

We included ORN cases that occurred in the mandibular molar region within a previously irradiated field and met the diagnostic criteria for ORN[5]. We included MRONJ cases with a history of treatment with bisphosphonates or denosumab who met the diagnostic criteria for MRONJ[7]. Cases who did not meet the diagnostic criteria for ORN or MRONJ were classified as having bacterial OM based on patient history. Among the 150 cases included in the study, 61 had bacterial OM, 19 had ORN, and 70 had MRONJ. Two of the 19 subjects with ORN also had a history of bisphosphonate treatment for osteoporosis. However, their disease was classified as ORN on the basis of the diagnostic criteria for ORN and MRONJ.

For the CT examinations, the MDCT device used was LightSpeed VCT (GE Healthcare, Chicago, IL), and after January 2023, Revolution Frontier (GE Healthcare, Chicago, IL) was used. The imaging conditions for LightSpeed VCT included a tube voltage of 120 kV, tube current of 330 mA or less (Auto mA), slice thickness of 0.625 mm, matrix size of 512 × 512, and a field of view (FOV) of 25 cm. For Revolution Frontier, the imaging conditions included a tube voltage of 80 and 140 kV (Dual energy), tube current of 600 mA, slice thickness of 0.625 mm, matrix size of 512 × 512, and FOV of 25 cm.

The dental CBCT equipment used was Alphard VEGA (Asahi Roentgen Ind Co., Ltd., Kyoto, Japan). The imaging conditions were set in P mode (tube voltage of 80 kV, tube current of 5 mA, slice thickness of 0.3 mm, matrix size of 512 × 512, and FOV of 15 cm) or I mode (tube voltage of 80 kV, tube current of 5 mA, slice thickness of 0.2 mm, matrix size of 512 × 512, and FOV of 10 cm).

The panoramic X-ray device used for panoramic X-ray examinations was Hyper-X (Asahi Roentgen Ind Co., Ltd., Kyoto, Japan). The imaging conditions included a tube voltage of 64 kV, tube current of 8 mA, and exposure time of 12 s.

The MRI equipment used for the MRI examinations was Signa HDxt 1.5 T (GE Healthcare, Chicago, IL), and after April 2023, Signa Premier 3.0 T (GE Healthcare, Chicago, IL) was used. Dedicated head and neck phased-array coils of 8 channels and 21 channels were used as transmit-receive coils, respectively. Imaging sequences included T1-weighted and T2-weighted fat-suppressed images. The MRI imaging conditions are presented in Table 7.

Imaging findings assessed

To categorize the imaging findings, the following features were evaluated by H.S., who has 20 years of experience as an oral and maxillofacial radiologist: (1) bone resorption, (2) osteosclerosis, (3) clarity of the mandibular canal, (4) periosteal reaction, (5) cortical bone perforation, (6) sequestrum (necrotic bone), and (7) pathological fracture. The results of the CT images were considered the gold standard for determining the presence or absence of each imaging finding. The detailed criteria for each diagnostic trait were as follows: (1) Bone resorption (Fig. 1): decreased CT values in the mandibular molar region compared with those in the contralateral region, an unaffected site on CT images, increased radiolucency in the same area on panoramic radiographs and clear bone resorption (bone defect) areas in T1- and T2-weighted fat-suppressed MR images. (2) Osteosclerosis (Fig. 2): Increased CT values in the mandibular molar region compared with the contralateral unaffected site on CT images, increased radiopacity in the same area on panoramic X-ray images, and clear areas of bone sclerosis in

	Signa HDxt 1.5 T		Signa premier 3.0 T	
	T1-wI	T2-wI	T1-wI	T2-wI
Repetition time (ms)	500	3600	500	3630
Echo time (ms)	7	80	7	80
Field of view (cm)	24			
Matrix size	256 × 256	256 × 256	416 × 384	320 × 224
Slice thickness (mm)	5			
Spacing (mm)	1			
Band width (kHz)	31.25	31.25	83.33	83.33
Number of excitations	1			
Echo Train Length	2	16	2	16
Scan time (ms)	1:14	2:03	1:38	1:49

Table 7. MRI imaging conditions. *T1-wI* T1-weighted images, *T2-wI* T2-weighted fat-suppressed images.

T1- and T2-weighted fat-suppressed MR images. (3) Clarity of the mandibular canal (Fig. 3): Clear visibility of the mandibular canal on CT images or panoramic radiographs compared with the unaffected contralateral site and clear visibility of the mandibular canal on T1- and T2-weighted fat-suppressed MR images. (4) Periosteal reaction (Fig. 4): Increased CT values outside the buccal, lingual or inferior cortex on CT images; increased radiopacity outside the inferior mandibular cortex on panoramic radiographs; and continuous areas of bone signal intensity outside the buccal, lingual or inferior cortex on T1- and T2-weighted fat-suppressed MR images. (5) Cortical bone perforation (Fig. 5): Discontinuity of the buccal, lingual or inferior cortex on CT images; discontinuity of the inferior mandibular cortex on panoramic radiographs; and discontinuity of the buccal, lingual or inferior cortex on T1- and T2-weighted fat-suppressed MR images. (6) Sequestrum (necrotic bone) (Fig. 6): Presence of bone islands with high CT values within the low-CT-value regions in the mandibular molar region on CT images, radiopacity within the radiolucency area in the mandibular molar region on panoramic radiographs, and no signal areas in the mandibular molar region on T1- and T2-weighted fat-suppressed MR images. (7) Pathological fracture (Fig. 7): presence of fracture lines and/or displacement of bone fragments on CT, panoramic, or T1- and T2-weighted fat-suppressed MR images.

For MRI analysis, signal intensities were evaluated on T1-weighted and T2-weighted fat-suppressed images and compared with those of the contralateral side. The areas of analysis included the mandibular bone marrow, masseter muscle, and parotid gland (Fig. 8). For T1-weighted and T2-weighted fat-suppressed images, we assessed the signal intensities within the mandibular bone marrow, masseter muscle, and parotid gland of the lesions and compared them with the signal intensities at the corresponding contralateral unaffected side.

Statistical analysis

For the age distribution of patients between disease groups, normality was examined via the Shapiro–Wilk test, with the significance level set at 5%. As groups with a significance level less than 5% were observed, they were considered not to follow a normal distribution. Therefore, the Kruskal–Wallis test was employed for analysis of variance, and in cases where significance was observed, Bonferroni's multiple comparison test was applied.

To investigate whether there were differences in the sex ratio of patients and the ratio of each imaging finding among bacterial OM, ORN, and MRONJ and to examine the association between the presence or absence of each imaging finding and the imaging modality, chi-square tests or Fisher's exact tests were conducted. When statistically significant differences were found among the three diseases ($p < 0.05$), to continue investigating differences between the two diseases, $p < 0.05/3$ was determined to be statistically significant by the Bonferroni correction in terms of multiple tests. With current sample sizes, the statistical power to detect overall differences, assuming a medium effect size (0.5) was > 0.99. For individual comparisons the statistical power was 0.81 (bacterial OM vs MRONJ), 0.48 (ORN vs. MRONJ) and 0.47 (bacterial OM vs. ORN). Statistical analysis was performed via SPSS ver. 22 (IBM Corp., Armonk, NY).

Conclusions

CT is an essential imaging tool for diagnosing OM/osteonecrosis in the jaw and is considered the gold standard for this diagnostic assessment. Diagnostic features include lytic and sclerotic changes, clarity of the mandibular canal, periosteal reactions, cortical bone perforation, sequestrum and pathological fractures. The relative frequencies of these findings were similar in bacterial OM and MRONJ but differed from those in ORN. Panoramic radiography is often used to evaluate these diseases. For detecting bone resorption and osteosclerosis, panoramic radiography has high diagnostic accuracy. However, MRI is more accurate than panoramic radiography for depicting periosteal reactions, cortical bone perforation, and sequestration. MRI also revealed the presence of bone marrow edema, an early change in these diseases.

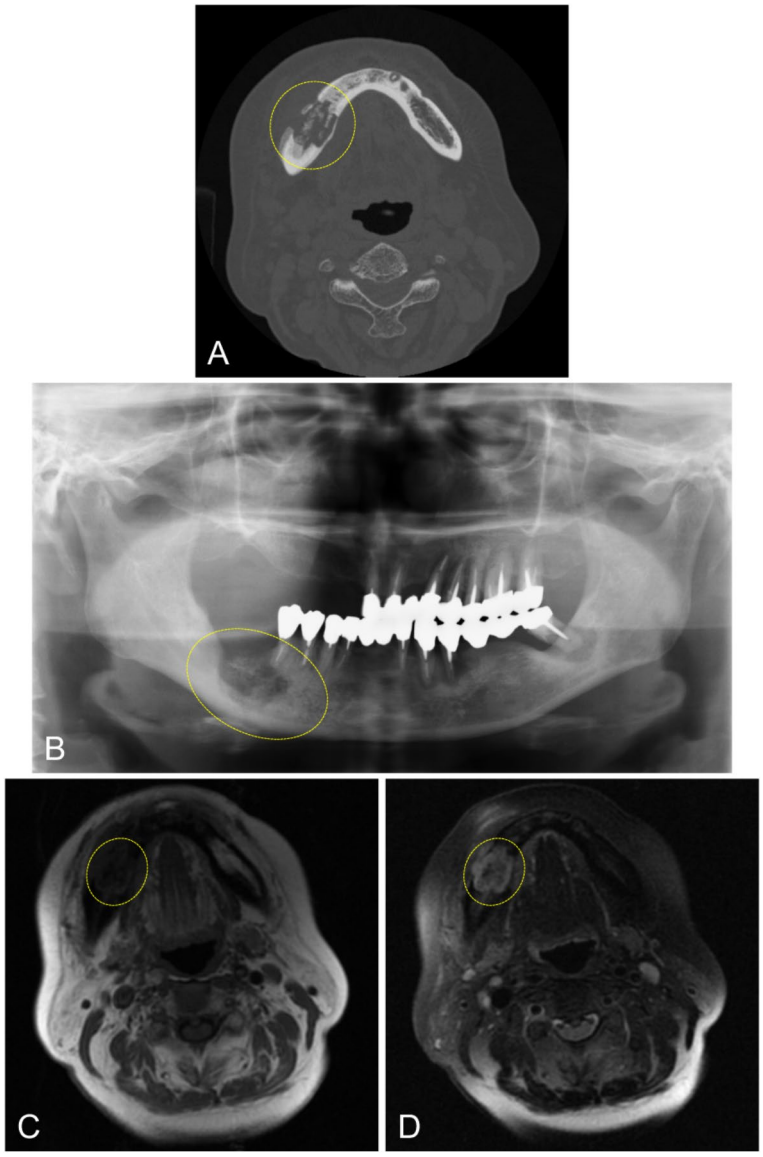

Fig. 1. Case with bone resorption. A 79-year-old female underwent extraction of the right mandibular first molar at a dental clinic. Upon investigation of medication due to incomplete healing of the extraction socket, it was revealed that she had been taking risedronate for osteoporosis for the past 3 years and alendronate for the past 1.5 years. She was then referred to our hospital for further treatment. (**A**) CT image (bone mode) showing a low CT value area in the trabecular bone of the right mandibular molar region (ellipse). (**B**) Panoramic X-ray image revealing radiolucency in the same area with surrounding sclerotic changes (ellipse). (**C**) T1-weighted MR image demonstrating the bone resorption area in the same region, with low signal intensity in the bone marrow compared with the contralateral side (ellipse). (**D**) T2-weighted fat-suppressed MR image demonstrating the bone resorption area in the same region, with high signal intensity in the bone marrow compared with the contralateral side (ellipse).

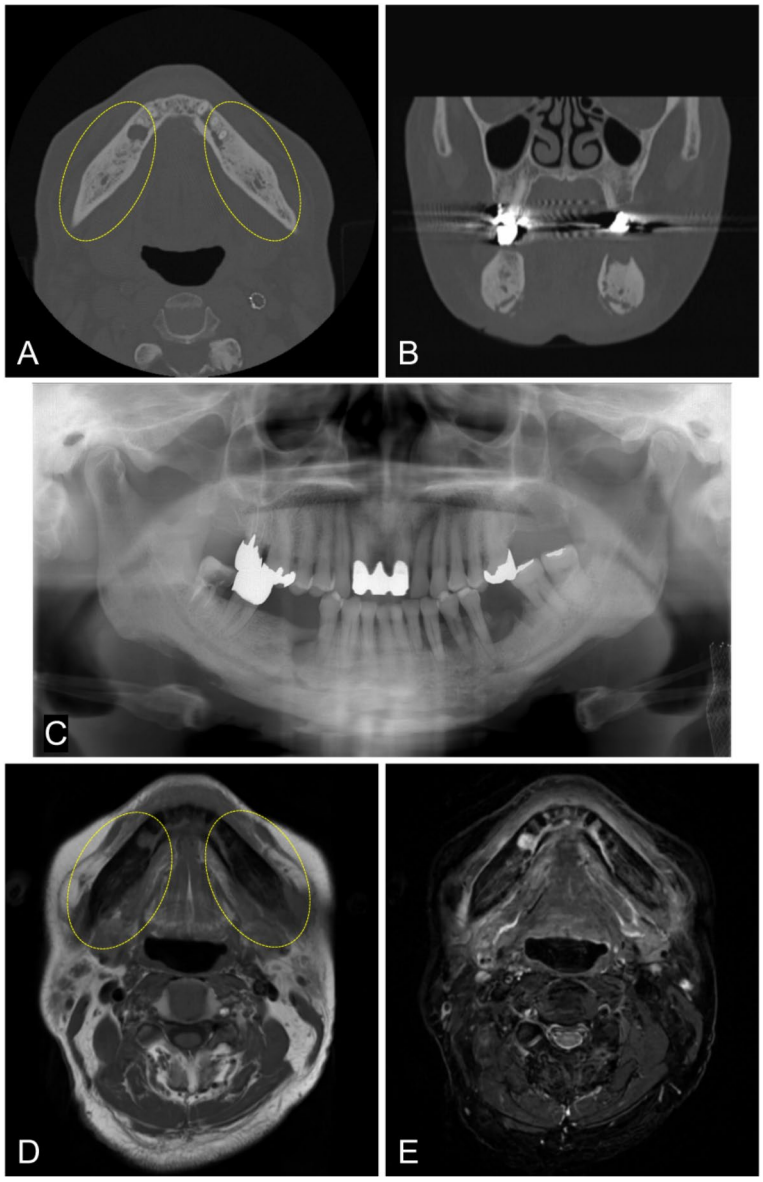

Fig. 2. Case with osteosclerosis. A 72-year-old male with a history of denosumab use for bone metastasis from bile duct cancer. Although he underwent extraction of the right mandibular second premolar at a dental clinic after a 2-month hiatus from medication, he was referred to our hospital due to treatment for bone exposure. (**A**, **B**) CT images (bone mode) showing an increase in CT values in the mandibular trabecular bone on both sides as well as the extraction socket of the right mandibular second premolar (ellipses). (**C**) Panoramic X-ray image revealing increased radiopacity in the mandibular trabecular bone on both sides. (**D**, **E**) T1-weighted MR image and T2-weighted fat-suppressed MR image demonstrate a sclerotic area in the same region, and the bone marrow signal in that area shows low signal intensity (ellipses).

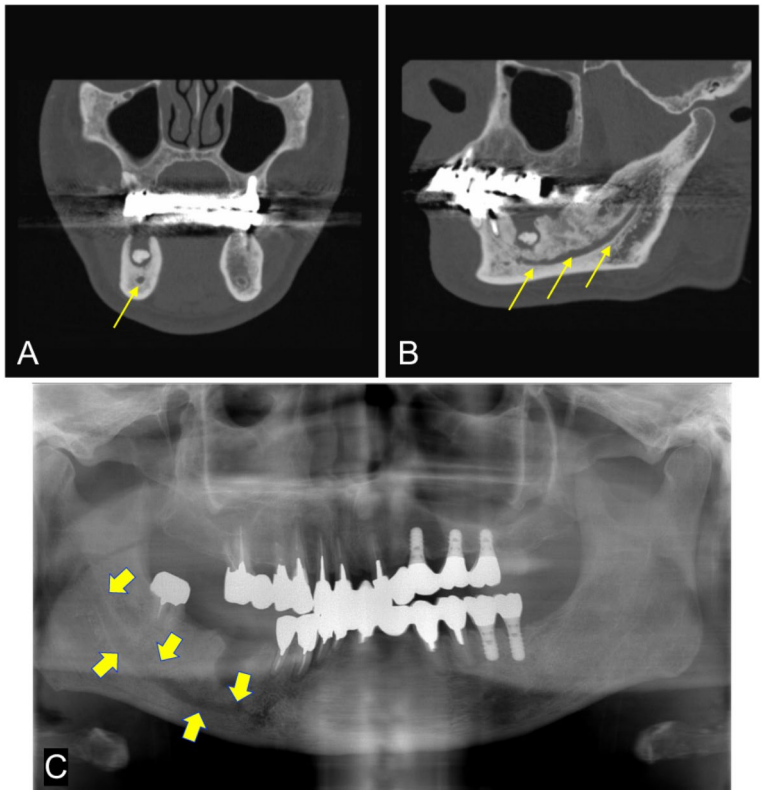

Fig. 3. Case with clarification of the mandibular canal. A 60-year-old male underwent extraction of the lower right first molar at a dental clinic. Pain and suppuration occurred in the same area, leading to a referral to our hospital. He was diagnosed with bacterial OM because of exclusion from the ORN or MRONJ criteria. (**A**, **B**) CT images (bone mode) showing clarification of the right inferior alveolar canal (arrows). (**C**) Panoramic X-ray image revealing similar findings (arrows). However, the results of MRI were inconclusive.

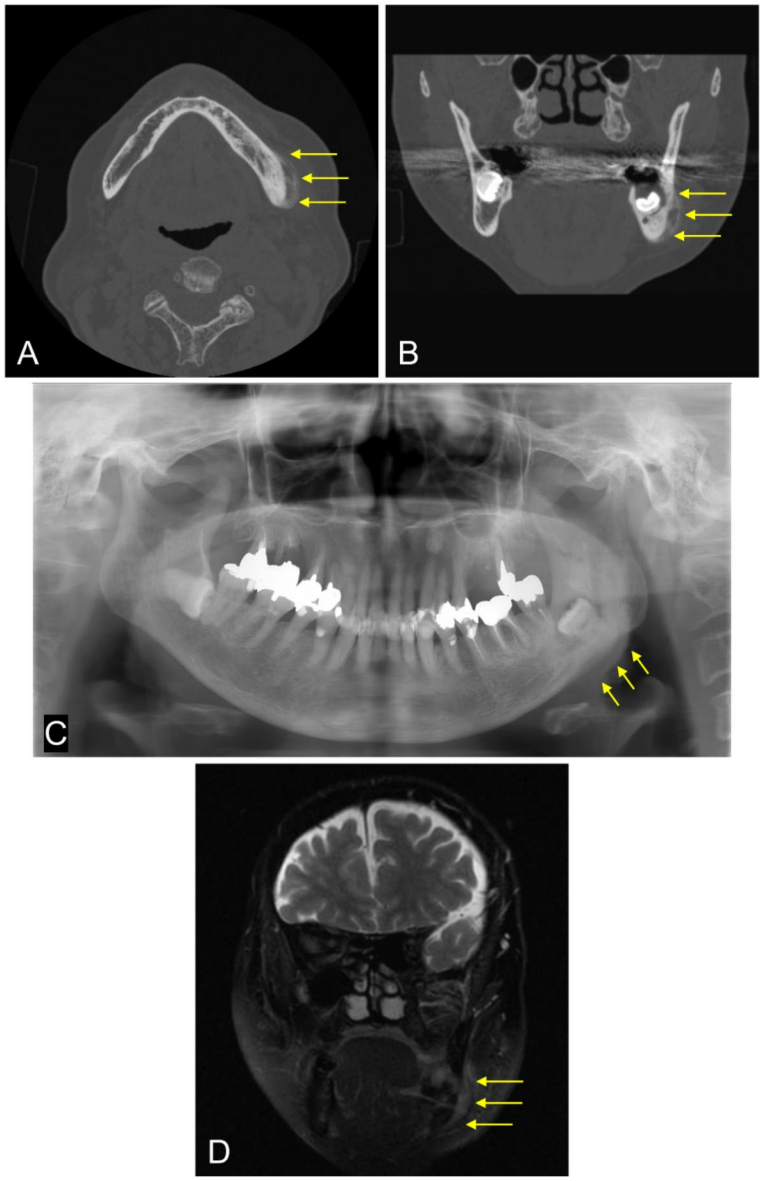

Fig. 4. Case with periosteal reaction. A 70-year-old female experienced discomfort in the lower left molar region and sought care at a dental clinic. Initially, she was informed about the impacted lower left third molar but was left untreated. Later, swelling in the area developed, leading to a referral to our hospital. She was diagnosed with bacterial OM because of exclusion from the ORN or MRONJ criteria. (**A**, **B**) The CT images (bone mode) showing an area of increased CT values continuous with the outer cortical bone (arrows). (**C**) Panoramic X-ray image revealing increased radiopacity (new bone formation) along the lower border of the mandible (arrows). (**D**) T2-weighted fat-suppressed MR image displaying a high signal intensity area continuous with the outer cortical bone (arrows).

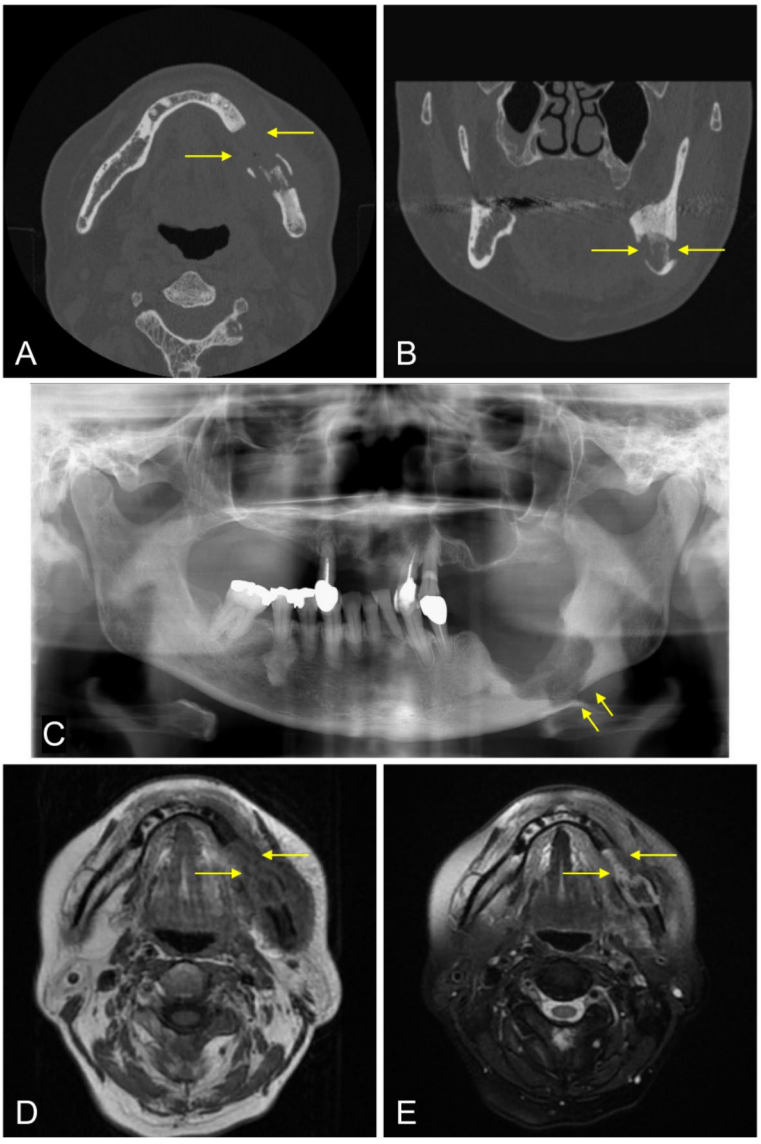

Fig. 5. Case with cortical bone perforation. A 64-year-old female had a history of using zoledronate for 3 years and pamidronate for 2 years to prevent bone metastasis from breast cancer. She was referred to our hospital due to swelling on the left side of the cheek and limited mouth opening. (**A**, **B**) CT images (bone mode) not showing continuity of the cortical bone on the buccal and lingual sides (arrows). (**C**) Panoramic X-ray image not revealing continuity of the cortical bone along the lower border of the mandible (arrows). (**D**, **E**) T1-weighted MR image and T2-weighted fat-suppressed MR image not showing continuity of the cortical bone on the buccal and lingual sides (arrows).

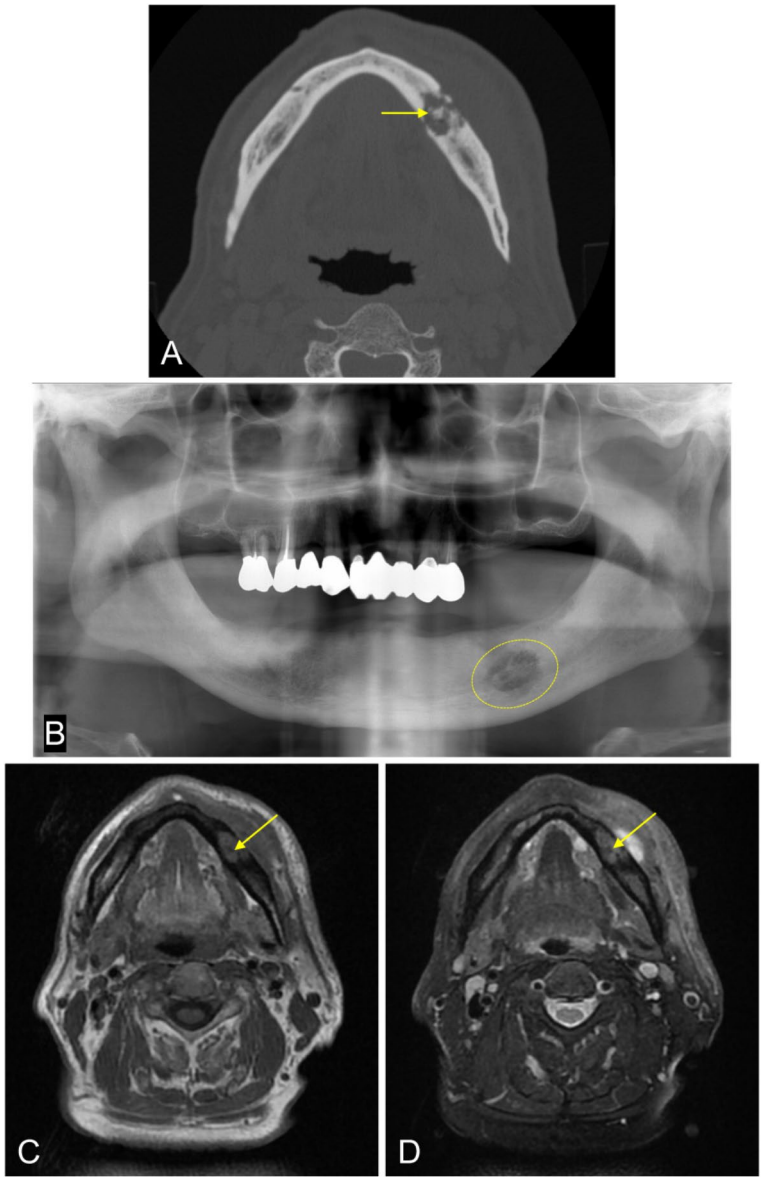

Fig. 6. Case with a sequestrum. An 81-year-old male underwent extraction of the left lower second premolar at a dental clinic. Nonhealing extraction socket complications persisted, with periods of improvement and worsening. CBCT imaging revealed sequestrum in the left mandibular molar region, leading to referral to our hospital. He was diagnosed with bacterial OM because of exclusion from the ORN or MRONJ criteria. (**A**) CT image (bone mode) showing islands of high CT values within the low CT value area (arrow). (**B**) Panoramic X-ray image revealing radiopaque areas within the radiolucent area (ellipse). (**C**, **D**) T1-weighted MR image and T2-weighted fat-suppressed MR image demonstrating no signal intensity region suspected to be sequestrum (arrows).

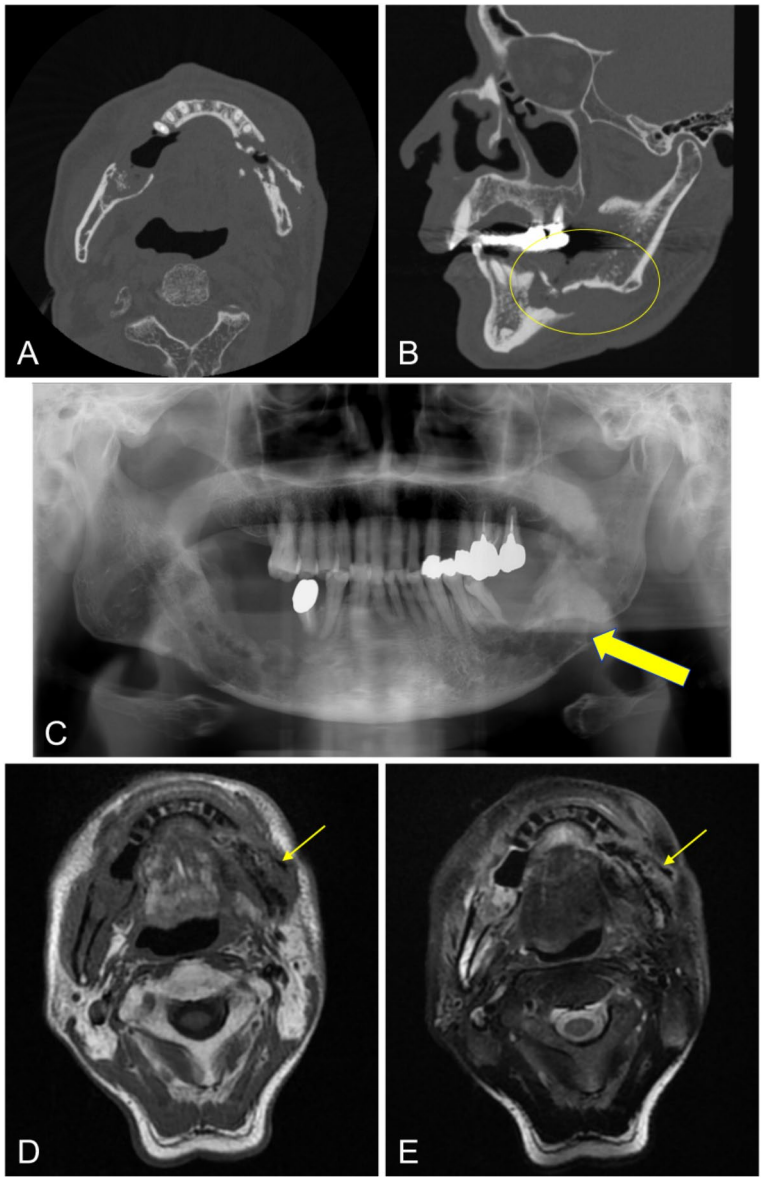

Fig. 7. Case with a pathological fracture. A 75-year-old male received chemoradiotherapy with 70 Gy for nasopharyngeal cancer. He subsequently developed radiation-induced osteomyelitis on both sides of the mandible. (**A**, **B**) CT images (bone mode) showing separation and displacement of the mandible in the region of the left lower molar (ellipse). (**C**, **D**, **E**) Panoramic X-ray images, T1-weighted MR images, and T2-weighted fat-suppressed MR images revealing separation and displacement of the mandible in the region of the left lower molar (arrows).

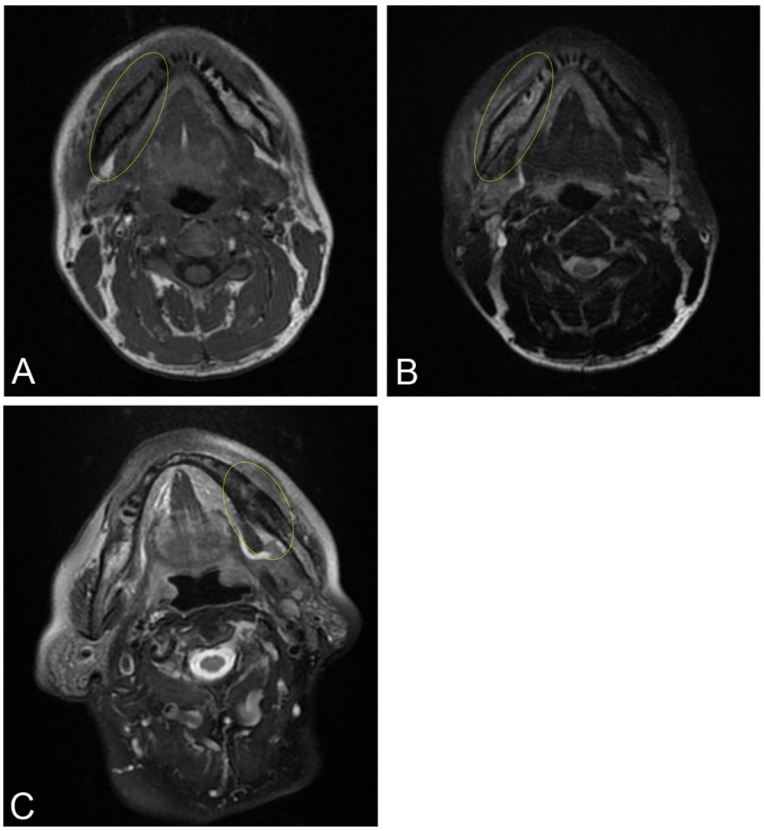

Fig. 8. Examples of MR signal intensities of lesions compared with those of the contralateral side. A 39-year-old male presented at a local clinic with pain and swelling on the right side of the mandible. Root canal treatment was performed on the right lower first molar, but the swelling did not improve. He also developed abnormal sensation of the mental nerve and was referred to our hospital. (**A**) T1-weighted image showing low signal intensity compared with the healthy side (ellipse). (**B**) T2-weighted fat-suppressed image showing high signal intensity compared with the healthy side (ellipse). An 86-year-old female presented at a local clinic with swelling in the left lower molar region of the mandible. She was treated with alendronate for osteoporosis and was referred to our clinic. (**C**) T2-weighted fat-suppressed image showing low signal intensity compared with the healthy side (ellipse).

Data availability

The datasets used and analyzed during the current study are available from the corresponding author on reasonable request.

Received: 25 September 2024; Accepted: 1 April 2025
Published online: 10 April 2025

References

1. Schmitt, S. K. Osteomyelitis. *Infect. Dis. Clin. North. Am.* **31**, 325–338 (2017).
2. Krakowiak, P. A. Alveolar osteitis and osteomyelitis of the jaws. *Oral Maxillofac. Surg. Clin. North. Am.* **23**, 401–413 (2011).
3. Otto, S. et al. Infection as an important factor in medication-related osteonecrosis of the jaw (MRONJ). *Medicina (Kaunas)* **57**, 1–12 (2021).
4. Schuknecht, B. & Valavanis, A. Osteomyelitis of the mandible. *Neuroimaging Clin. N. Am.* **13**, 605–618 (2003).
5. Chronopoulos, A., Zarra, T., Ehrenfeld, M. & Otto, S. Osteoradionecrosis of the jaws: definition, epidemiology, staging and clinical and radiological findings. A concise review. *Int. Dent. J.* **68**, 22–30 (2018).
6. Chrcanovic, B. R., Reher, P., Sousa, A. A. & Harris, M. Osteoradionecrosis of the jaws-a current overview-part 1. *Oral Maxillofac. Surg.* **14**, 3–16 (2010).
7. Ruggiero, S. L. et al. American association of oral and maxillofacial surgeons' position paper on medication-related osteonecrosis of the jaws—2022 update. *J. Oral Maxillofac. Surg.* **80**, 920–943 (2022).
8. Tanaka, R. & Hayashi, T. Computed tomography findings of chronic osteomyelitis involving the mandible: Correlation to histopathological findings. *Dentomaxillofac. Radiol.* **37**, 94–103 (2008).
9. Qaisi, M. & Montague, L. Bone margin analysis for osteonecrosis and osteomyelitis of the jaws. *Oral Maxillofac. Surg. Clin. North. Am.* **29**, 301–313 (2017).
10. Tsuchimochi, M. & Kurabayashi, T. Symposium: Imaging modalities for drug-related osteonecrosis of the jaw (1), role of imaging in drug-related osteonecrosis of the jaw: An up-to-date review (secondary publication). *Jpn. Dent. Sci. Rev.* **55**, 1–4 (2019).
11. Reinert, C. P. et al. [18F]Fluoride positron-emission tomography (PET) and [18F]FDG PET for assessment of osteomyelitis of the jaw in comparison to computed tomography (CT) and magnetic resonance imaging (MRI): A prospective PET/CT and PET/MRI pilot study. *J. Clin. Med.* **11**, 3998 (2022).

12. Schulze, D., Blessmann, M., Pohlenz, P., Wagner, K. W. & Heiland, M. Diagnostic criteria for the detection of mandibular osteomyelitis using cone-beam computed tomography. *Dentomaxillofac. Radiol.* **35**, 232–235 (2006).
13. Omami, G. The moth-eaten mandible: Osteomyelitis. *Ear Nose Throat J.* **102**, NP398–NP399 (2021).
14. Baba, A. et al. CT imaging features of antiresorptive agent-related osteonecrosis of the jaw/medication-related osteonecrosis of the jaw. *Dentomaxillofac. Radiol.* **47**, 20170323 (2018).
15. Posadzy, M., Desimpel, J. & Vanhoenacker, F. Cone beam CT of the musculoskeletal system: Clinical applications. *Insights Imaging* **9**, 35–45 (2018).
16. Lee, K. et al. Magnetic resonance imaging of normal and osteomyelitis in the mandible: Assessment of short inversion time inversion recovery sequence. *Oral Surg. Oral Med. Oral Pathol. Oral Radiol. Endod.* **96**, 499–507 (2003).
17. Orimo, H. et al. Japanese 2011 guidelines for prevention and treatment of osteoporosis-executive summary. *Arch. Osteoporos.* **7**, 3–20 (2012).
18. Cancer Information Service. Cancer Statistics in Japan 2024. https://ganjoho.jp/public/qa_links/report/statistics/pdf/cancer_statistics_2024_fig_E.pdf (2024).
19. Bolouri, C. et al. Performance of orthopantomography, planar scintigraphy, CT alone and SPECT/CT in patients with suspected osteomyelitis of the jaw. *Eur. J. Nucl. Med. Mol. Imaging.* **40**, 411–417 (2013).
20. Strobel, K. et al. Stellenwert der SPECT/CT zur abklärung von kiefererkrankungen. *Radiologe* **52**, 638–645 (2012).
21. Shuster, A. et al. Comparison of the histopathological characteristics of osteomyelitis, medication-related osteonecrosis of the jaw, and osteoradionecrosis. *Int. J. Oral Maxillofac. Surg.* **48**, 17–22 (2019).
22. De Antoni, C. C. et al. Medication-related osteonecrosis of the jaw, osteoradionecrosis, and osteomyelitis: A comparative histopathological study. *Braz. Oral Res.* **32**, e23 (2018).
23. Bury, D. C., Rogers, T. S. & Dickman, M. M. Osteomyelitis: Diagnosis and treatment. *Am. Fam. Physician.* **104**, 395–402 (2021).
24. Lee, Y. J., Sadigh, S., Mankad, K., Kapse, N. & Rajeswaran, G. The imaging of osteomyelitis. *Quant. Imaging Med. Surg.* **6**, 184–198 (2016).
25. Pineda, C., Espinosa, R. & Pena, A. Radiographic imaging in osteomyelitis: The role of plain radiography, computed tomography, ultrasonography, magnetic resonance imaging, and scintigraphy. *Semin. Plast. Surg.* **23**, 80–89 (2009).
26. Fritz, J. M. & McDonald, J. R. Osteomyelitis: Approach to diagnosis and treatment. *Physician Sportsmed.* **36**, 50–54 (2008).
27. Offiah, A. C. Acute osteomyelitis, septic arthritis and discitis: Differences between neonates and older children. *Eur. J. Radiol.* **60**, 221–232 (2006).
28. Tiwari, P., Bera, R. N., Kanojia, S., Chauhan, N. & Hirani, M. S. Assessing the optimal imaging modality in the diagnosis of jaw osteomyelitis. A meta-analysis. *Br. J. Oral Maxillofac. Surg.* **59**, 982–992 (2021).
29. Bianchi, S. D., Scoletta, M., Cassione, F. B., Migliaretti, G. & Mozzati, M. Computerized tomographic findings in bisphosphonate-associated osteonecrosis of the jaw in patients with cancer. *Oral Surg. Oral Med. Oral Pathol. Oral Radiol. Endod.* **104**, 249–258 (2007).
30. Stockmann, P. et al. Panoramic radiograph, computed tomography or magnetic resonance imaging. Which imaging technique should be preferred in bisphosphonate-associated osteonecrosis of the jaw? A prospective clinical study. *Clin. Oral. Investig.* **14**, 311–317 (2010).
31. Mardini, S. & Gohel, A. Imaging of odontogenic infections. *Radiol. Clin. North. Am.* **56**, 31–44 (2018).
32. Reinert, S., Widlitzek, H. & Venderink, D. J. The value of magnetic resonance imaging in the diagnosis of mandibular osteomyelitis. *Br. J. Oral Maxillofac. Surg.* **37**, 459–463 (1999).
33. Wongratwanich, P. et al. Do various imaging modalities provide potential early detection and diagnosis of medication-related osteonecrosis of the jaw? A review. *Dentomaxillofac. Radiol.* **50**, 20200417 (2021).
34. García-Ferrer, L. et al. MRI of mandibular osteonecrosis secondary to bisphosphonates. *Am. J. Roentgenol.* **190**, 949–955 (2008).
35. Zhou, A. K. et al. Radiological evaluation of postoperative osteomyelitis in long bones: Which is the best tool?. *J. Perioper. Pract.* **32**, 15–21 (2022).
36. Schumann, P. et al. Correlation of dynamic contrast-enhanced bone perfusion with morphologic ultra-short echo time MR imaging in medication-related osteonecrosis of the jaw. *Dentomaxillofac. Radiol.* **51**, 20210036 (2022).
37. Muraoka, H. et al. Efficacy of diffusion-weighted magnetic resonance imaging in the diagnosis of osteomyelitis of the mandible. *Oral Surg. Oral Med. Oral Pathol. Oral Radiol.* **133**, 80–87 (2022).
38. Baba, A. et al. Symposium: Imaging modalities for drug-related osteonecrosis of the jaw (4), CT and MR imaging findings of antiresorptive agent-related osteonecrosis of the jaws/medication-related osteonecrosis of the jaw (secondary publication). *Jpn. Dent. Sci. Rev.* **55**, 58–64 (2019).
39. Obinata, K. et al. Image findings of bisphosphonate related osteonecrosis of jaws comparing with osteoradionecrosis. *Dentomaxillofac. Radiol.* **46**, 20160281 (2017).
40. Ogura, I. et al. Tc-99m hydroxymethylene diphosphonate scintigraphy, computed tomography, and magnetic resonance imaging of osteonecrosis in the mandible: Osteoradionecrosis versus medication related osteonecrosis of the jaw. *Imaging Sci. Dent.* **49**, 53–58 (2019).
41. Akashi, M. et al. Differences between osteoradionecrosis and medication-related osteonecrosis of the jaw. *Oral Maxillofac. Surg.* **22**, 59–63 (2018).
42. Mallya, S. M. & Tetradis, S. Imaging of radiation- and medication-related osteonecrosis. *Radiol. Clin. North. Am.* **56**, 77–89 (2018).

Author contributions

M.K., H.S., and S.M. contributed to the study design. H.S., N.Y., N.T., and Y.U. performed the data acquisition. H.S., A.T., and T.T. analyzed the data. H.S., S.K., S.M.M., F.G.Y., and S.M. contributed to data interpretation. M.K., H.S. and D.A.N. contributed to writing the original draft. All authors critically revised the manuscript, gave final approval, and agreed to be accountable for all aspects of the work.

Declarations

Competing interests

The authors declare no competing interests.

Additional information

Supplementary Information The online version contains supplementary material available at https://doi.org/10.1038/s41598-025-96910-x.

Correspondence and requests for materials should be addressed to H.S.